Iterative Impedance Learning Control for Ankle Rehabilitation

Kun Qian, Zhiqiang Zhang, Samit Chakrabarty, and Shengquan Xie *

Abstract

In this paper, impedance learning control is investigated for conducting robot-aided ankle rehabilitation. Under repetitive interaction tasks, the ankle dynamic is described as a time-varying iterative system with unknown mechanical impedance parameters. The gradient following approach and iterative learning algorithm are employed to obtain a desired impedance model. With learned parameters, an inner torque controller with robot dynamic compensation is implemented for tracking the modified trajectory. Experimental results with an ankle rehabilitation robot prototype validate the efficacy of proposed method.

1. Introduction

Ankle joint plays a decisive role in standing, ambulation and balancing, but it is highly susceptible to neurological and musculoskeletal injury [1]. Physiotherapy is essential for rehabilitation of ankle motion function and it necessitates labour and intensive leading efforts by the physiotherapists. Robot-aided therapy is a promising field that provides long-term repetitive environment, accurate sensing and reliable records [2–4]. Differ from industrial scenario, rehabilitation-aided robot must be configured for stable, safe and compliant motion in contact with human. However, unknown and dynamical changes of the human ankle bring along difficulties to interaction controller design [5].

The impedance control proposed by Hogan [6] has been considered as one of the most powerful interaction control methods. The objective of this control concept is to accomplish a desired mechanical impedance at robot end-effector. However, employing predefined impedance model tends to be conservative, and a better interaction performance can be expected with other choices [7, 8]. Moreover, numerous industrial applications are mainly aimed at rigid interaction objects which can be characterized by stationary impedance parameters [9–11]. The human ankle dynamics, however, is continuously changing and highly individual-dependent [12]. Learning process is common in motion-based tasks, for instance, when a person pushes the footboard forward, he/she may fail in the beginning due to lack of interaction knowledge, e.g. mass, inertia and fraction of the footboard. After several repetitions, the person learns a better set of impedance parameter of his/her ankle while desired target is achieved as long as the control effort will be minimized.

To reproduce such human inspired learning process in interaction controller design, many variable impedance control (VIC) schemes have been proposed. Position-based VICs have been proposed in [13–15] with force senseless approach, and the impedance model is modified by end-effector velocity at each portion of task. With force sensor feedback, control schemes in [16, 17] adjust model parameters by constructing an auxiliary interaction force dynamic. However, these methods have an inherent trade-off for position error and iterative force that have limited performance. To mimic the intelligent decision-making process and the physical behaviour pattern of human operators, neutral network and fuzzy algorithms are utilized to determine and change the robot impedance during the task [18–20]. Nevertheless, the considerable computation costs and offline training cycles bring difficulties to real-time implementation. In addition, existing VICs are rarely validated on rehabilitation robotics and how to fully utilize the repetitive characteristic of tasks is still open.

This paper proposes a learning impedance controller for enhancing interaction performance when conducting robot-aided ankle rehabilitation. By virtue of the repetitive rehabilitation tasks, the interaction process is described as a linear time-varying repetitive system. The gradient following method that decreasing a multiple interaction index is introduced, and impedance parameters are iteratively adjusted such that the desired impedance model is learned despite unknown ankle dynamics. A PD-based torque controller with robot dy-
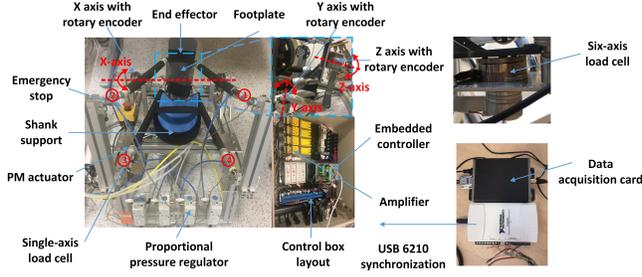
1

Figure 1: The CARR with three rotational DOFs.

namic compensation is employed to conduct interaction task, and participant involved experiments on an ankle robot prototype verify the efficacy of the proposed controller.

2. Problem formulation

2.1. Ankle Rehabilitation Robot

Fig. 1 presents the compliant ankle rehabilitation robot (CARR) developed by our group [21, 22]. Three rotational DOFs for ankle plantarflexion/dorsiflexion, inversion/eversion and adduction/abduction, are denoting as X, Y and Z axis, respectively. Four compliance pneumatic muscle (PM) actuators are adopted for providing driving torque, while rotary encoders, single-axis load cells and six-axis load-cell are implemented for measuring angular displacement, PM pulling force and interactive torque, respectively.

Consider the human ankle interacting with the CARR, the human-robot dynamics can be modelled by

$$M(q)\ddot{q} + C(q,\dot{q})\dot{q} + G(q) = \tau_r - \tau_h \qquad (1)$$

where $q \in \mathbb{R}^3$ is the angle vector; $M(q) \in \mathbb{R}^{3\times3}$, $C(q,\dot{q})\dot{q} \in \mathbb{R}^3$ and $G(q) \in \mathbb{R}^3$ denote inertia matrix, centripetal and Coriolis torque and gravity vector, respectively; $\tau_r \in \mathbb{R}^3$ is the control torque and $\tau_h \in \mathbb{R}^3$ is the human-robot interactive torque.

Assume that the individual is controlling the mechanical impedance of his/her ankle joint that producing the similar trajectory of the robot. The ankle's dynamics can be described by the following mass-damping-spring model

$$M_h\ddot{q} + B_h\dot{q} + K_h q = \tau_h \qquad (2)$$

where $M_h \in \mathbb{R}^{3\times3}$, $B_h \in \mathbb{R}^{3\times3}$ and $K_h \in \mathbb{R}^{3\times3}$ are inertia, damping and spring matrices, which are all diagonal and positive definite. Unlike stationary interaction, different individuals have divergent configuration

for the ankle joint that implies M_h, B_h and K_h are unknown. Moreover, movement adaption is also common in human joint motion that brings time-varying property to the impedance parameters. Therefore, using fixed impedance parameters for controller design is unconscionable under rehabilitation scenario.

2.2. Control Objective

The objective of this work is to achieve better interaction control when conducting robot-aided ankle rehabilitation. In particular, we follow a standard impedance control procedure with the target impedance model

$$M_d(\ddot{q}_d - \ddot{q}) + B_d(\dot{q}_d - \dot{q}) + K_d(q_d - q) = \tau_h \qquad (3)$$

where $M_h \in \mathbb{R}^{3\times3}$, $B_h \in \mathbb{R}^{3\times3}$ and $K_h \in \mathbb{R}^{3\times3}$ are target impedance parameter matrices and $q_d \in \mathbb{R}^3$ is the desired trajectory. For an enhanced interaction, we need to find proper M_d, B_d and K_d that match the human joint model in (2). By virtue of the task repetition during rehabilitation, an iterative adaption law is proposed for seeking impedance parameter with previous selection and current feedback. The updating criteria is to minimize a cost function J^k (reinforcement) at $k \in \mathbb{N}^+$ iteration which will be specified later. The parameter learning laws take the following forms

$$\Delta M_d^k = \eta_M(J^k), \ \Delta B_d^k = \eta_B(J^k), \ \Delta K_d^k = \eta_K(J^k) \quad (4)$$

where $\eta_M(J^k)$, $\eta_B(J^k)$ and $\eta_K(J^k)$ are feedback learning terms that contains different components of J^k. ΔM_d^k, ΔM_d^k and ΔM_d^k are the difference of parameter between two consecutive iterations. The initial value M_d^0, B_d^0 and K_d^0 can be selected according to ankle dynamic baseline. With learned impedance parameters, a modified trajectory q_d^k at k-th iteration is derived by

$$M_d^k(\ddot{q}_d - \ddot{q}_d^k) + B_d^k(\dot{q}_d - \dot{q}_d^k) + K_d^k(q_d - q_d^k) = \tau_h. \quad (5)$$

Then, the torque control method is developed to make $q \to q_d^k$ in time interval $t \in [0, T], \forall k$. Note that only the modified trajectory will be redefined in (3), while the feedback information within current iteration is used to evaluate J^k. The proposed control architecture with outer impedance parameter learning and inner torque control is given in Fig. 2.

3. Controller Design

3.1. Iterative Impedance Learning

Since arbitrary selection of M_d may cause instability, M_d is fixed with apparent ankle inertia and only B_d
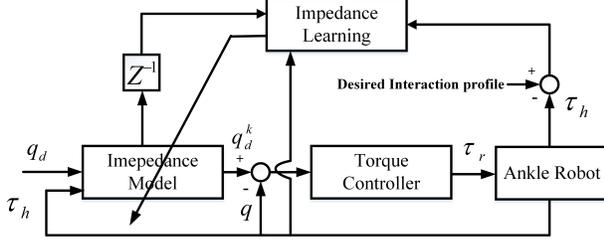
Figure 2: Block diagram of the iterative impedance learning controller.

and K_d are learned during rehabilitation. The gradient following method [23] is employed for iteratively decreasing J^k which update B_d^k and K_d^k by

$$\Delta B_d^k = -\alpha_B (\frac{\partial J^k}{\partial B_d^k})^T = -\alpha_B (\frac{\partial \tau_h^k}{\partial B_d^k})^T (\frac{\partial J^k}{\partial \tau_h^k})^T \quad (6)$$

$$\Delta K_d^k = -\alpha_K (\frac{\partial J^k}{\partial K_d^k})^T = -\alpha_K (\frac{\partial \tau_h^k}{\partial K_d^k})^T (\frac{\partial J^k}{\partial \tau_h^k})^T \quad (7)$$

where α_B and α_K are learning rates. From (3), we have $(\frac{\partial \tau_h^k}{\partial B_d^k})^T = \dot{q}_d^T - \dot{q}^{kT} = \dot{e}^{kT}$ and $(\frac{\partial \tau_h^k}{\partial K_d^k})^T = q_d^T - q^{kT} = e^{kT}$. Due to the unknown ankle dynamics, the derivative $(\frac{\partial J^k}{\partial \tau_h^k})^T$ in (6) and (7) is not available. To overcome this problem, various reinforcement algorithms for estimating the derivative have been proposed [18,20,23]. Take advantage of the repetitive nature of rehabilitation, we propose an alternative way via iterative learning concept that do not require explicit knowledge of ankle dynamics and aforementioned estimation processes.

To introduce iterative learning concept, we first rewrite (2) into state-space form

$$\begin{bmatrix} \dot{x}_1 \\ \dot{x}_2 \\ \dot{x}_3 \end{bmatrix} = \begin{bmatrix} 0 & I & 0 \\ -M_h^{-1}K_h & -M_h^{-1}B_h & 0 \\ 0 & 0 & 0 \end{bmatrix} \begin{bmatrix} x_1 \\ x_2 \\ x_3 \end{bmatrix} + \begin{bmatrix} 0 \\ -M_h^{-1} \\ I \end{bmatrix} \tau_h \quad (8)$$

where $x_1 = q$, $x_2 = \dot{q}$, $x_3 = \int_0^T \tau_h(s)ds$ and I is the unit matrix with proper dimension. By denoting $X = \begin{bmatrix} x_1 \\ x_2 \\ x_3 \end{bmatrix}$,

$A = \begin{bmatrix} 0 & I_n & 0 \\ -M_h^{-1}K_h & -M_h^{-1}B_h & 0 \\ 0 & 0 & 0 \end{bmatrix}$ and $B = \begin{bmatrix} 0 \\ -M_h^{-1} \\ I_n \end{bmatrix}$,

along with the time-varying property discussed in Section 2.1, we transfer the ankle dynamic model (2) into the following linear time-varying system

$$\dot{X} = A(t)X + B(t)\tau_h$$
$$Y = C(t)X \quad (9)$$

where $C(t)$ denotes the relationship between the states (i.e. position, velocity and integration of interactive torque) and the output Y. The following Lemma formalises a result for implementing a D-type ILC on system (9).

Lemma 1 [24]. *Consider the following LTV system works in an iterative manner*

$$\dot{X}^k = A(t)X^k + B(t)u^k$$
$$Y^k = C(t)X^k. \quad (10)$$

Suppose that control input u^k is iteratively updated as

$$u^k = u^{k-1} + \Gamma(\dot{Y}_d - \dot{Y}^k) \quad (11)$$

where Y_d is a realizable desired output and learning gain Γ satisfies

$$||I - \Gamma C(t)B(t)|| < 1. \quad (12)$$

If $C(t)B(t)$ is full-column rank and identical initial condition $Y^k(0) = Y_d(0)$ is satisfied, uniform convergence of output tracking is guaranteed. That is, $Y^k \to Y_d$ uniformly in $t \in [0,T]$ as $k \to \infty$.

According to Lemma 1, the following updating law is constructed by taking τ_h in (9) as control input

$$\tau_h^k = \tau_h^{k-1} - \Gamma(\dot{Y}^k - \dot{Y}_d) \quad (13)$$

which indicates that τ_h is updated for iteratively decreasing the error between Y^k and Y_d. Approximately, we define this error as the cost function J^k, and measure by $J^k = ||Y^k - Y_d||_2$, where $||\cdot||$ denotes two-norm. Notice that all components of Y^k are available from feedback measure. Similar to the gradient following approach, we obtain

$$\tau_h^k = \tau_h^{k-1} - \alpha_\tau (\frac{\partial J^k}{\partial \tau_h^k})^T. \quad (14)$$

Comparing (13) and (14), the derivative can be approximated by

$$\frac{\partial J^k}{\partial \tau_h^k} = \frac{\Gamma}{\alpha_\tau}(\dot{Y}^k - \dot{Y}_d)^T. \quad (15)$$

Substituting (15) to (6) and (7), we obtain the learning law

$$\Delta B_d^k = B_d^k - B_d^{k-1} = -\frac{\alpha_B}{\alpha_\tau}\Gamma \dot{e}^k(\dot{Y}^k - \dot{Y}_d)^T$$

$$\Delta K_d^k = K_d^k - K_d^{k-1} = -\frac{\alpha_K}{\alpha_\tau}\Gamma e^k(\dot{Y}^k - \dot{Y}_d)^T. \quad (16)$$

Remark 1. *Parameter learning law (16) take simple form, which is developed based on feedback measures from the interaction task instead of modelling the human ankle. The output gain $C(t)$ plays a vital role in constructing the error based cost function J^k which represents the weight between position, velocity and interactive torque.*
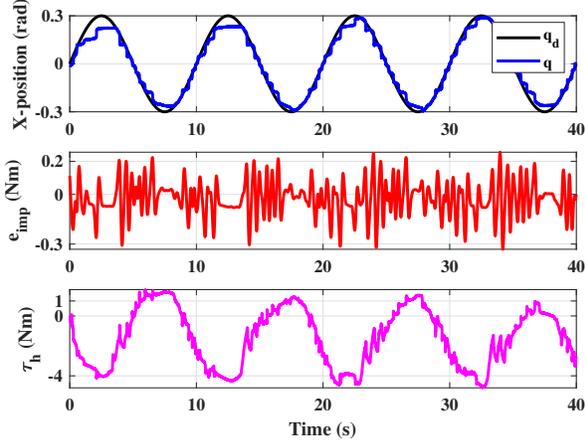
Figure 3: Trail of S1 with only inner torque control.

Figure 4: Trail of S2 with only inner torque control.

3.2. Torque Control via Force Distribution

The learned parameters B_d^k and K_d^k have been obtained through the outer-loop impedance learning, the modified trajectory q_d^k is obtained according to (5). Thus, an inner torque controller is developed in this section to make $q \to q_d^k$. We construct the following control law that combines with the error feedback and compensation of robot dynamics

$$
\begin{aligned}
\tau_r =& \Lambda_p e + \Lambda_v \dot{e} + M(q)\ddot{q}_d^k + C(q,\dot{q})\dot{q}_d^k \\
& + G(q) + \tau_h
\end{aligned}
\tag{17}
$$

where Λ_p and Λ_v are two positive control gains. By defining Lyapunov candidate $V = \frac{1}{2}\dot{e}^T M(q)\dot{e} + \frac{1}{2}e^T \Lambda_p e$ and adopting property $\frac{1}{2}\big(\dot{M}(q) - 2C(q,\dot{q})\big)$ is skew-symmetric, the stability analysis follows [25]. So far, the control torque (17) is designed to make $\dot{e} \to 0$ in $t \in [0,T]$. Unlike conventional motor-driven rehabilitation robot, CARR utilizes PM as actuator for an enhanced compliance. If PM is not fully in tension, instability may occur which requires conducting force distribution from designed control torque (17) to individual actuator force. To fulfil this potential problem, an analytic-iterative force distribution technique [26] is implemented by solving following optimization problems

$$
\min_y f(y) = (F_0 + Ay)^T (F_0 + Ay)
$$

$$
\text{s.t. } F_{\min} - (F_0 + Ay) \le 0
\tag{18}
$$

where y is the optimal solution; $F_0 = (J^T)^\dagger F_m$ with Jacobian matrix J^T and measured actuator force F_m; $A = $ orthonormal$\{I - (J^T)^\dagger J^T\}$ and F_{min} is a non-negative constant.
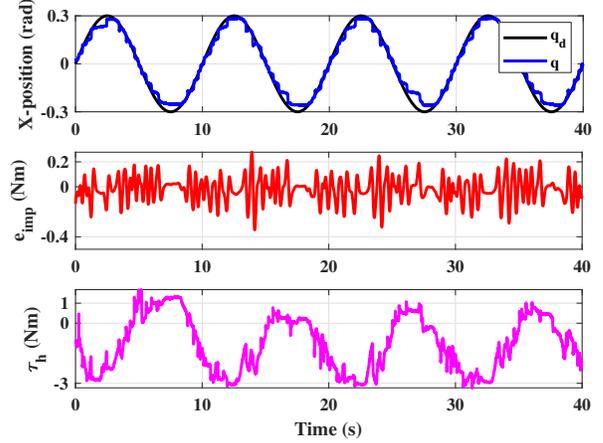
Remark 2. *The CARR is a self-developed prototype with explicit knowledge of model parameters, thus, we construct (17) by involving direct model compensations. Notice that adaptive/robust control schemes can also be applied in the inner loop for further need.*

4. Experimental Results

Experiments are conducted with two human participants (S1 and S2) that have been approved by the University of Leeds Research Ethics Committee (reference MEEC 18-001). During experiments, desired interaction torque is set to zero indicating that the ankle robot is trying to minimize participants' effort, i.e., reinforcing compliance. Note that variable interaction profile can also be applied using proposed impedance learning approach. We are here using ankle passive impedance for verification, and more active and resistive training scenarios will be conducted further. The desired trajectory is defined as

$$
q_d = \begin{bmatrix} 0.3\sin(2\pi f t) \\ 0 \\ 0 \end{bmatrix}
\tag{19}
$$

where $f = 0.1$. The initial impedance parameter in (5) are set as $M_d^0 = 0.01$, $B_d^0 = 2$ and $K_d^0 = 40$ according to [12]. To verify the validity of impedance learning scheme, the outer learning loop is first disabled and the tracking results with only torque controller are shown in Fig. 3 and 4. Each trail contains four repetitive trajectories, i,e, $q_d^k = q_d$, $k = 1,2,3,4$, and feedback gains in (17) are set as $\Lambda_p = 30$ and $\Lambda_v = 5$. The error between actual interaction toque and desired impedance dynamic is defined as

$$
e_{\text{imp}} = M_d^0 \ddot{e}^k + B_d^0 \dot{e}^k + K_d^0 e^k - \tau_h.
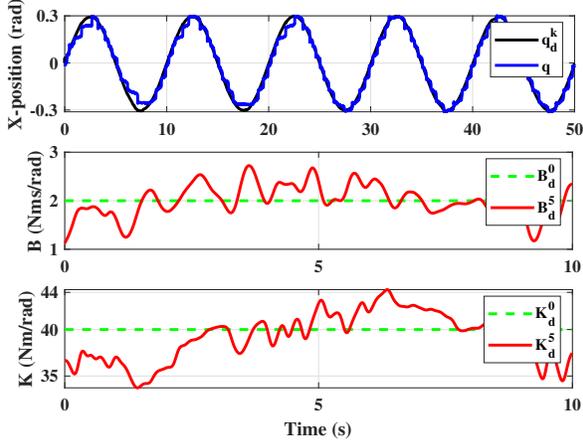\tag{20}
$$

4

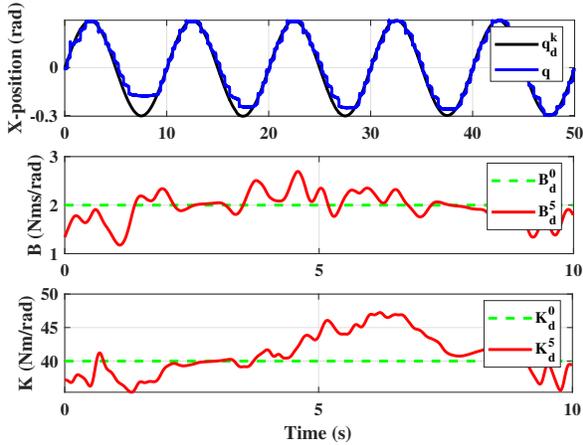Figure 5: Trail of S1 with iterative impedance learning.

Figure 6: Trail of S2 with iterative impedance learning.

We can observe that for both S1 and S2, the position tracking is satisfactory that can almost follow the desired trajectory. Due to the existing of impedance error, such position error cannot be eliminated. A discussed in Section 2, the predefined impedance parameters is part of the reason for limited interaction performance. Also, the interaction torque of both subjects have similar tendency with different magnitude that demonstrates the individual-dependent property.

Subsequently, the iterative impedance learning controller is then tested. The learning gain in (16) are set as $\frac{\alpha_B}{\alpha_\tau} = 2$, $\frac{\alpha_K}{\alpha_\tau} = 5$ and $\Gamma = 8$. The output gain in (9) is set as $C(t) = [10\ 0\ 1]$ and $Y_d = \begin{bmatrix} q_d^k \\ \dot{q}_d^k \\ 0 \end{bmatrix}$ that gives $J^k = ||10e^k - \int_0^T \tau_h(s)ds||_2$. For a fair comparison, feedback gains Λ_p and Λ_v remain unchanged. The initial
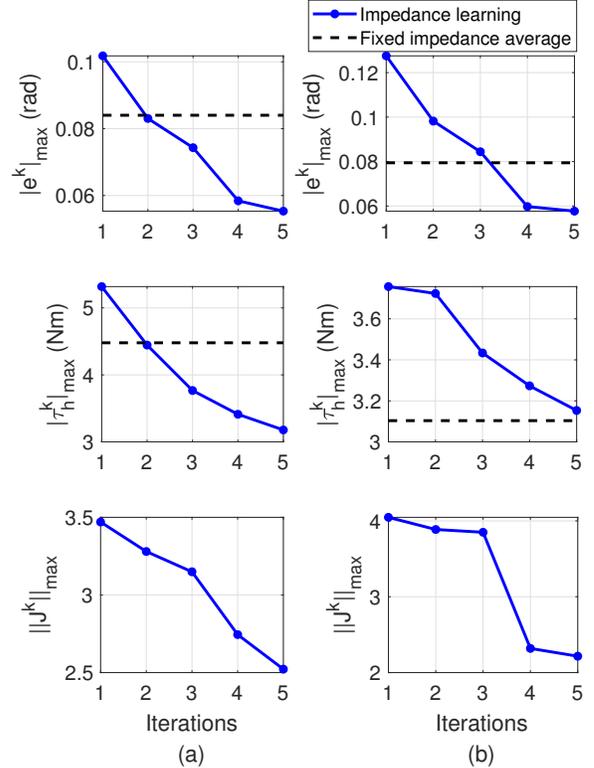

Figure 7: Convergence curves of position error, interaction force and cost function. (a) S1; (b) S2.

value of impedance parameter is utilized in first iteration as baseline, and also four repetitive trajectories are conducted after. The performance for S1 and S2 are shown in Fig. 5 and 6, and the learned parameter after 4 iterations are also given. It can be seen that both position tracking performance are gradually enhanced as learning process is ongoing. Besides, impedance parameters after learning is different indicating that proposed learning law is able to capture the individual of subjects' ankle dynamic.

To further illustrate the learning process, convergence curves for position error, interaction force and cost function are given in Fig. 7. The dotted lines are average value in the first experiment with fixed initial impedance parameters. For both subjects, the position errors have been effectively reduced by 8% within four iterations. With selected output gain $C(t)$, the expectation of effective decreasing of position error is validated. The interaction torque for S1 has also been reduced, however, there is not a big improvement for S2. Furthermore, the convergence of cost function is different for S1 and S2, indicating that arbitrary selection of leaning gain may degrade the control performance due to disparate interaction profiles.

5. Conclusion

In this paper, an iterative impedance learning controller is proposed for conducting repetitive ankle training. A two-loop structure is constructed with outer impedance learning and inner torque control. By describing the ankle dynamics as a time-varying system, an iterative leaning law with gradient following approach is introduced. Experimental results on the CARR illustrate the effectiveness of proposed controller. In the followed work, different selection of learning rate α_B and α_K, output gain $C(t)$ and more iterations of training require further investigation.

References

[1] C. G. Mattacola and M. K. Dwyer, "Rehabilitation of the ankle after acute sprain or chronic instability," *J. Athl. Training*, vol. 37, no. 4, p. 413, 2002.

[2] H. I. Krebs, N. Hogan, M. L. Aisen, and B. T. Volpe, "Robot-aided neurorehabilitation," *IEEE Trans. Rehabil. Eng.*, vol. 6, no. 1, pp. 75–87, 1998.

[3] P. K. Jamwal, S. Hussain, Y. H. Tsoi, and S. Q. Xie, "Musculoskeletal model for path generation and modification of an ankle rehabilitation robot," *IEEE Trans. Human-Mach. Syst.*, vol. 50, no. 5, pp. 373–383, 2020.

[4] X. Li, Q. Yang, and R. Song, "Performance-based hybrid control of a cable-driven upper-limb rehabilitation robot," *IEEE Trans. Biomed. Eng.*, vol. 68, no. 4, pp. 1351–1359, 2020.

[5] K. Jalaleddini, E. S. Tehrani, and R. E. Kearney, "A subspace approach to the structural decomposition and identification of ankle joint dynamic stiffness," *IEEE Trans. Biomed. Eng.*, vol. 64, no. 6, pp. 1357–1368, 2016.

[6] N. Hogan, "Impedance control: An approach to manipulation: Part i—theory," 1985.

[7] S. P. Buerger and N. Hogan, "Complementary stability and loop shaping for improved human–robot interaction," *IEEE Trans. Robot.*, vol. 23, no. 2, pp. 232–244, 2007.

[8] F. Ferraguti, N. Preda, and A. Manurung, "An energy tank-based interactive control architecture for autonomous and teleoperated robotic surgery," *IEEE Trans. Robot.*, vol. 31, no. 5, pp. 1073–1088, 2015.

[9] C. Yang, G. Peng, Y. Li, R. Cui, L. Cheng, and Z. Li, "Neural networks enhanced adaptive admittance control of optimized robot–environment interaction," *IEEE Trans. Cybern.*, vol. 49, no. 7, pp. 2568–2579, 2018.

[10] E. Arefinia, H. A. Talebi, and A. Doustmohammadi, "A robust adaptive model reference impedance control of a robotic manipulator with actuator saturation," *IEEE Trans. Syst., Man, Cybern., Syst.*, vol. 50, no. 2, pp. 409–420, 2017.

[11] L. Liu, S. Leonhardt, C. Ngo, and B. J. Misgeld, "Impedance-controlled variable stiffness actuator for lower limb robot applications," *IEEE Trans. Autom. Sci. Eng.*, vol. 17, no. 2, pp. 991–1004, 2019.

[12] H. Lee, E. J. Rouse, and H. I. Krebs, "Summary of human ankle mechanical impedance during walking," *IEEE J. Transl. Eng. Health Med.*, vol. 4, pp. 1–7, 2016.

[13] R. V. Dubey, T. F. Chan, and S. E. Everett, "Variable damping impedance control of a bilateral telerobotic system," *IEEE Control Syst. Mag.*, vol. 17, no. 1, pp. 37–45, 1997.

[14] M. S. Erden and A. Billard, "Robotic assistance by impedance compensation for hand movements while manual welding," *IEEE Trans. Cybern.*, vol. 46, no. 11, pp. 2459–2472, 2015.

[15] F. Ficuciello, L. Villani, and B. Siciliano, "Variable impedance control of redundant manipulators for intuitive human–robot physical interaction," *IEEE Trans. Robot.*, vol. 31, no. 4, pp. 850–863, 2015.

[16] H.-P. Huang and S.-S. Chen, "Compliant motion control of robots by using variable impedance," *Int. J. Adv. Manuf. Tech.*, vol. 7, no. 6, pp. 322–332, 1992.

[17] A. Taherifar, G. Vossoughi, and A. Selk Ghafari, "Optimal target impedance selection of the robot interacting with human," *Adv. Robot.*, vol. 31, no. 8, pp. 428–440, 2017.

[18] H. Modares, I. Ranatunga, F. L. Lewis, and D. O. Popa, "Optimized assistive human–robot interaction using reinforcement learning," *IEEE Trans. Cybern.*, vol. 46, no. 3, pp. 655–667, 2015.

[19] F. Dimeas and N. Aspragathos, "Fuzzy learning variable admittance control for human-robot cooperation," in *IROS. 2014*, 2014, pp. 4770–4775.

[20] Z. Du, W. Wang, Z. Yan, W. Dong, and W. Wang, "Variable admittance control based on fuzzy reinforcement learning for minimally invasive surgery manipulator," *Sensors*, vol. 17, no. 4, p. 844, 2017.

[21] W. Meng, S. Q. Xie, Q. Liu, C. Z. Lu, and Q. Ai, "Robust iterative feedback tuning control of a compliant rehabilitation robot for repetitive ankle training," *IEEE/ASME Trans. Mechatronics*, vol. 22, no. 1, pp. 173–184, 2016.

[22] M. Zhang, J. Cao, G. Zhu, Q. Miao, X. Zeng, and S. Q. Xie, "Reconfigurable workspace and torque capacity of a compliant ankle rehabilitation robot (CARR)," *Robot. Auton. Syst.*, vol. 98, pp. 213–221, 2017.

[23] B.-H. Yang and H. Asada, "Progressive learning and its application to robot impedance learning," *IEEE Trans. Neural Netw.*, vol. 7, no. 4, pp. 941–952, 1996.

[24] S. S. Saab, "A discrete-time stochastic learning control algorithm," *IEEE Trans. Autom. Control*, vol. 46, no. 6, pp. 877–887, 2001.

[25] J.-J. E. Slotine and W. Li, "On the adaptive control of robot manipulators," *Int. J. Robot. Res.*, vol. 6, no. 3, pp. 49–59, 1987.

[26] M. Hassan and A. Khajepour, "Analysis of bounded cable tensions in cable-actuated parallel manipulators," *IEEE Trans. Robot.*, vol. 27, no. 5, pp. 891–900, 2011.